

Resonant x-ray emission spectra of Mn based Heusler alloys.

M.V. Yablonskikh^{1,2}, Yu.M. Yarmoshenko,² I.V. Solovyev^{2,3}, L. Gridneva⁴, T.

Schmitt¹, M. Magnuson¹, L.-C. Duda¹, E.Z. Kurmaev² and J. Nordgren¹

¹*Department of Physics, Uppsala University, Angstrom Laboratory, Box 530, S-75121 Uppsala, Sweden*

²*Institute of Metal Physics, Russian Academy of Sciences-Ural Division, 620219 Yekaterinburg, GSP-170, Russia*

³*Joint Research Center for Atom Technology, c/o NAIR, 1-1-4 Higashi, Tsukuba 305-0046, Japan and*

⁴*MAXLAB, Lund University, P.O.Box 118, S-22100, Lund, Sweden*

The Mn L_2, L_3 x-ray spectra of the Cu_2MnAl and Co_2MnZ ($Z=\text{Al, Ga, Sn, Sb}$) Heusler alloys have been investigated by the Resonant X-ray Emission Spectroscopy (RXES) using linearly polarized monochromatic synchrotron radiation for. The interplay between the half-metallic character of the Mn 3d electronic structure in connection with the local magnetic moment μ_{Mn} and Mn $2p \rightarrow 3d$ x-ray emission spectra is discussed.

PACS numbers: 78.70. En, 75.25.+z, 75.20 Hr, 87.64 Ni

I. INTRODUCTION

The interest to Mn based Heusler alloys [1] is connected with the problem of half-metallic ferromagnets (HMF) [2]. These materials have an energy gap for one of the spin projections at the Fermi level and represent a separate class of strong itinerant magnetic substances. The "classical" alloys of this type are PtMnSb and NiMnSb mostly known as half-metallic ferromagnets with the lattice structure $C1_b$. Searching the substances with similar properties it was found the X_2MnZ Heusler alloys with the crystal lattice $L2_1$ where X is for example Fe, Co, Ni, Pd, Rh and Z is Al, Ga, Si, Sn, Sb, In are proposed to be also promising for magnetic applications [2]. Mn-based Heusler alloys are particularly interesting because of their compatibility with existing semiconductor technology. The remarkable feature is a high magnetic moment (3-4.6 μ_B), that is mainly being formed by Mn atoms [3]-[4]. So, the electronic structure of the half-metallic ferromagnets and related materials allows them to be efficiently applied as a source of spin-polarized charge carriers [5].

In case of the X_2MnZ the $L2_1$ structure is slightly modified comparing to $C1_b$, that, however, affects the electronic structure i.e. of Mn atoms in a different ways depending on the type of X and Z elements. The influence to the type of the magnetic ordering has been predicted and explained mainly because of changes in intra-atomic distances between the atoms. In particular that effects the minority-spin electrons to make them lose their semiconducting character, while the majority-spin electrons keep to stay metallic [6]. Thereby it is important to understand the interplay between the electronic structure of Mn and magnetic characteristics of Heusler alloys searching for relation between the formation of the strong, almost 100% spin-polarized structure of the conduction electrons and the chemical type of the X and Z element. The chance to study topic has been given by x-ray emission spectroscopy technique using the ability to extract the element selective information about the valence structure and detecting the x-ray transitions lo-

calized to the first coordination sphere. We applied the method to study of the Mn L_2, L_3 x-ray emission spectra excited by linearly polarized monochromatic synchrotron radiation studying $2p_{1/2} \rightarrow 3d_{3/2}$ and $2p_{3/2} \rightarrow 3d_{3/2,5/2}$ photon emission transitions respectively for the line of alloys Cu_2MnAl , Co_2MnZ ($Z=\text{Al, Ga, Sn, Sb}$) in order to investigate the interplay between the local magnetic moment at Mn site, alterations in the Mn 3d band structure and the experimental Mn $L_{2,3}$ x-ray emission spectra.

II. EXPERIMENTAL SETUP

The samples investigated are polycrystallines used before at the series of experiments both by x-ray photoelectron [7, 8] and x-ray emission spectroscopy [9]. The present experiment was performed at the bulk branch line of beamline I511 at MAX II (MAX-lab National Laboratory, Sweden). The x-ray absorption (XA) spectra were measured by recording the total electron yield (TEY) using the scanning the photon energy of the incident monochromatized synchrotron radiation. TEY absorption spectra were recorded by measuring sample drain current. The XA spectra were normalized to the photo current from a clean gold mesh introduced into the synchrotron radiation beam in order to correct for intensity variations of the incident x-ray beam. The soft x-ray emission (XE) spectra were recorded with a high-resolution Rowland-mount grazing-incidence grating spectrometer [10] with a two-dimensional detector. The monochromator energy band pass used for all XA spectra and for the excitation of the RXE spectra was approximately 0.15 eV and 0.25 eV respectively. At beam line I511 (MAX II) refocusing optics situated in front of the measurement chamber and focusing the beam down to a vertical beam size of below 20 μ is being used. The angle of the incident photon beam was about 5°, while spectrometer had been set perpendicularly in a horizontal plane. The selected grating and the entrance slit value lead to the 1.0 eV resolution of the spectra detected. The vacuum was below $2 - 3 \cdot 10^{-9}$ Torr.

III. RESULTS

The measured XA spectra are displayed at the Fig.1. They are been looking almost identical to each other. We found the such spectra are typical of divalent Mn, that indicated the metallic character of the chemical bonding. Presented XA spectra are seems to be almost similar to each other. Contradictory to that the dependence of the XE spectra for every excitation energy has some differences from each other. First let pay attention to spectra at the Fig.2(a) excited with L_3 absorbtion edge excitation energy $E_{exc}=641$ eV. The only Mn L_3 x-ray emission line is to be excited at that case. One can easily distinguish two-peak structure at the region 635-642 eV, where the heights position in the energy scale have been selected as *A* and *B*.

For the case of excitation energy $E_{exc}=644$ eV displayed at the Fig.2(b) the two-peak structure is observed also. The energy position of them is the same like in case Fig.2(a). The intensity of the peak *B* relative to peak *A* $I(B)/I(A)$ is to be the same for Cu_2MnAl and Co_2MnAl but is being increased in line Co_2MnZ from $Z=\text{Al}$ to $Z=\text{Sb}$. The dependence is valid both for all cases presented at the Fig.2 for both excitation energies *a* and *b* selected below the L_2 absorbtion edge. The elastic peak with half-width about 0.3 eV is not crossed with the energy region of the peak *B* with position at 641 eV in photon energy scale. Note the $I(B)/I(A)$ ratio is growing up in line of alloys for the case *a*, Fig.2(a), so we still have $I(B)/I(A)$ dependence in a line Co_2MnAl , Co_2MnZ from $Z=\text{Al}$ to $Z=\text{Sb}$.

Next we will pay attention to the spectra excited with energies near the Mn L_2 absorbtion edge, Fig.3(a),(b). The non-resonant spectra excited with $E_{exc}=670$ eV are shown at the Fig.3(c). The dependence of the $I(L_2)/I(L_3)$ ratio in line of alloys Cu_2MnAl , Co_2MnAl and to Co_2MnSb is observed, which is similar for $I(B)/I(A)$ ratio. The two-peak structure of the L_3 line can not be distinguished because of the excitation energy selected far enough from the L_3 absorbtion edge. The dependencies of the $I(B)/I(A)$ and $I(L_2)/I(L_3)$ from the alloy type are summarized at the Fig.4.

The electronic structure calculations in the local-spin-density approximation have been performed using the linear muffin-tin orbital method.[11] The atomic spheres radii for X, Mn and Z were chosen from the charge neutrality condition inside the spheres, and using the experimental lattice parameters. The Brillouin zone integration was performed using the linear tetrahedron method and 172 nonequivalent \mathbf{k} -points (corresponding to the 14:14:14 devisions of the reciprocal lattice vectors for the face-centered cubic structure). State densities are given at Fig.5 for X_2MnAl ($\text{X}=\text{Co}$ and Cu) and at Fig.6 for Co_2MnZ ($Z=\text{Ga}$, Sn , Sb). Here \uparrow designates the majority-spin electrons and \downarrow the minority-spin electrons. The minority-spin state densities at the Fermi energy for Mn in Co_2MnZ are nearly vanished. Estimated magnetic moments (Table.I) are in a good agreement with experi-

mental ones.

IV. DISCUSSION

First the general terms using for the spectroscopy data will be briefly mentioned. At the second, the attention will be given to the calculations and conclusions related. Finally we will finish with the explanation of the experimental results, considering the task to not exactly identify the mechanism of the forming Mn $L_{2,3}$ spectra in Heusler alloys, but to find out and describe the correlation between magnetic properties of the materials, electronic structure of the Mn 3d in alloys and respective x-ray emission spectra.

The shape of the L_3 emission line $2p_{3/2} \rightarrow 3d_{5/2,3/2}$ reflects 3d DOS only indirectly, first because of the general nature of the process of resonant/non-resonant photon scattering. In order to understand the complication of the principal ability of the spectra formation exactly for Mn $L_{3,2}$ one can look into recent work by F. Borgatti *et.al.* [12]. In order to avoid the point of discussion from the general discussion of the elastic and inelastic x-ray scattering in soft x-ray region that is supposed to be the separate branch of studies, we will focus mostly at the relative changes at x-ray spectra.

Relating to the experience of x-ray emission studies already been done for the Mn $L_{2,3}$ of the Co_2MnSb , NiMnSb using the magnetic circular dichroism the terms of "normal" emission and "re-emission" has to be only briefly introduced. By "normal" emission one can understand the $2p \rightarrow 3d$ transition created by the radiative relaxation of the 3d electron from the *occupied* part of DOS to the 2p core hole. By "re-emission" the same radiative relaxation of the 3d electron excited to the *unoccupied* part of DOS is defined. Looking at the Figs.2 one can distinguish these impacts to the Mn L_3 spectra: the peak *A* corresponds to "normal" emission impact and the peak *B* corresponds to the "re-emission" of the Mn 3d electron from *unoccupied* to the Mn $2p_{3/2}$ core hole.

At the Fig.5 calculations of the Cu_2MnAl and Co_2MnAl are presented. The Me 3d majority-spin electrons in case of Co are more delocalized then in Cu case. The value of the Mn 3d density of states $N(E_F)_{\downarrow}$ for Mn minority-spin projection is significantly lower in case of Co_2MnAl comparing to Cu_2MnAl , see TableI. In line of the Co_2MnZ where Z is being changed from $Z=\text{Al}$ to $Z=\text{Sb}$, the the *Co* 3d and Mn 3d DOS structures are similar to each other for the current alloy, see Fig.6. The value of the $N(E_F)_{\downarrow}$ is diminished in line $Z=\text{Al}$, Ga , Sn , Sb , that means the Mn 3d DOS becomes close to the half-metallic state following the line mentioned.

It is not possible to pass over the systematic calculations performed for Fe_2MnZ ($Z = \text{Al}, \text{Si}, \text{P}$)[13]. The option discovered for this line tells about the ability to make Mn 3d DOS structure half-metallic, changing the Z element. That shows principal ability to reach the half-metallic state of the DOS changing the chemical type of

the third element in X_2MnZ . The similar role of Z atom was also demonstrated experimentally [14, 15]. That is in a good agreement with results performed for the Cu_2MnAl and Co_2MnZ ($Z=Al, Ga, Sn$) [6] and with presented calculations.

Now we will focus on the explanation of the dependencies presented at the Fig.4 for the Co- Heusler alloys. Let us pay attention to the Fig.4 and data from the Table I. In line Co_2MnZ ($Z=Al, Ga, Sn, Sb$) where the dependence of the $I(B)/I(A)$ intensity ratio for the each excitation energy at and above the L_3 Mn absorption edge exists. The re-emission peak intensity grows with the decrease of the $N(E_F)_\downarrow$. The conclusion coming proposes the re-emission as an indicator of the closeness of the Mn 3d band to the half-metallic state.

The $I(L_2)/I(L_3)$ ratio is also growing in the same line of Co-alloys with $Z=Al, Ga, Sn, Sb$ comparing to that one in pure Mn. We have no such a transparent explanation of that. The promising way seems to consider Coster-Kronig impact in the redistribution of the L_3, L_2 intensities. The Coster-Kronig is supposed to be suppressed for the Mn in Heusler alloys that is found to be opposite for the case of pure Mn [8], but we cannot estimate the actual impact of the process in current case.

One can not also exclude the possibility of the re-emission to be involved in the formation of Mn L_2 x-ray spectra, that here is the radiative relaxation of the 3d electron from unoccupied part of Mn 3d DOS to the Mn $2p_{1/2}$ core hole. The conclusion one can make in this case is the connection between the growth of the $I(L_2)/I(L_3)$ ratio and the degeneration of the $N(E_F)_\downarrow$ value for the Z changing from Al to Sb in line of Co- alloys. We hope that experimental fact to be explained lately and be accepted as a observed.

The numerical values at the graph at Fig.4 make us believe in the existing correlation of the $I(B)/I(A)$ and the $I(L_2)/I(L_3)$ ratios with the value of the magnetic moment μ_{Mn} in line of Co_2MnZ , where Z is changing in order Al, Ga, Sn, Sb.

The situation becomes more complicated with the consideration of the Mn $L_{2,3}$ XE-spectra of Cu_2MnAl in connection with data for Co- Heusler alloys. The numerical values of the $I(B)/I(A)$ and the $I(L_2)/I(L_3)$ for X_2MnAl alloys are almost the same. Due to the suggested mechanism of the L_3 spectra formation $I(B)/I(A)$ should be much smaller for Cu_2MnAl , because of the $N(E_F)_\downarrow$ is much higher for Cu_2MnAl then for Co_2MnAl . There is also no correlation between the intensity ratios $I(B)/I(A)$, $I(L_2)/I(L_3)$ and μ_{Mn} for the Cu_2MnAl , Co_2MnAl group having different both μ_{Mn} and a lattice parameter, Fig.4, Table.I. The same μ_{Mn} and a values had been measured for the Cu_2MnAl , Co_2MnSb , but the $I(B)/I(A)$ and $I(L_2)/I(L_3)$ parameters are different for alloys.

According to that it is difficult to declare the transparent correlation between the dependence of the $I(L_2)/I(L_3)$, $I(B)/I(A)$ with both values of the μ_{Mn} and the $N(E_F)_\downarrow$ values for the X_2MnZ where Z is constant

element. The strong difference of Me 3d and Mn 3d band in case of Co- alloys and Cu- alloy could be a reason for that. The correlation is to be valid in the case X_2MnZ alloys, where Z is changing with the constant metal X.

V. CONCLUSION

There are several leads to be expressed. It was found the relative intensity of re-emission channel to be intensive and dependent on the value of the density of states at the Fermi level for the minority spin states in the half-metallic alloys of X_2MnZ type, where X metal is to be constant. Both the growth of the re-emission impact in forming Mn L_3 spectrum and $I(L_2)/I(L_3)$ ratio are connected with the decrease of the $N(E_F)_\downarrow$ value.

Having an example of the Cu_2MnAl and Co_2MnAl one can suggest that such a simple experimental approach of the estimation the gap value to be not functional in case of the replacement of the X - metal in X_2MnZ Heusler alloys. That is connected with a strong hybridization impact from Me $3d \uparrow$ and Mn $3d \uparrow$ states.

The result being shown could be used as a basis to continue the experiments with linearly or circularly polarized synchrotron radiation defining not only energy distribution of the scattered photons, but the overall intensity for the different excitation energies.

VI. ACKNOWLEDGMENT

Support from the Royal Swedish Academy of Sciences for cooperation between Sweden and the former Soviet Union is gratefully acknowledged. We would like to thank M. Katsnelson for the fruitful discussion and MAX-Lab National Laboratory staff for experimental support.

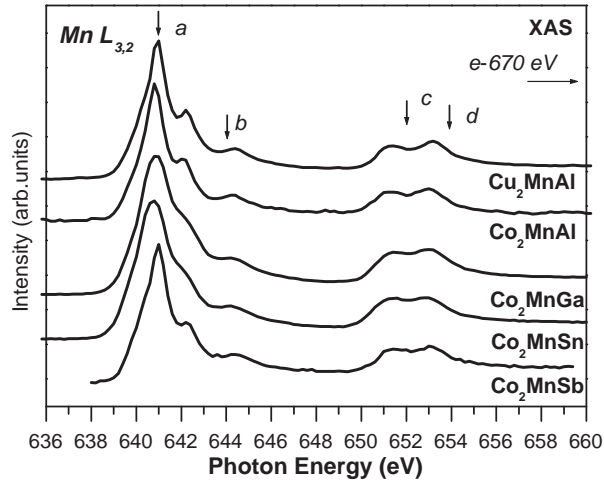


FIG. 1: XAS spectra. The excitation energies for resonant x-ray emission measurements are shown by the arrows

-
- [1] F. Heusler, Verh. Dtsch. Phys. Ges. **5**, 219 (1903).
 [2] R. D. Groot, F. Mueller, P. V. Engen, and K. Buschow, PRL **50**, 2024 (1983).
 [3] P. J. Webster and R. S. Tebble, Phil. Mag **16**, 347 (1967).
 [4] S. Ishida, S. Fujii, S. Kawhiwagi, and S. Asano, J. Phys. Soc. Jpn. **64**, 2152 (1995).
 [5] G. A. de Wijs1 and R. A. de Groot, Phys. Rev. B **64**, 020402(R) (2002).
 [6] J. Kübler, A. Williams, and C. Sommers, PRB **28**, 1745 (1983).
 [7] Y. Yarmoshenko *et al.*, Europ. Phys Journal B **2**, 1 (1998).
 [8] S. Plogmann *et al.*, Phys. Rev. B **60**, 6428 (1999).
 [9] M. V. Yablonskikh *et al.*, Phys. Rev. B **63**, 235117 (2001).
 [10] J. Nordgren *et al.*, Rev. of Sc. Inst. **60**, 1690 (1989).
 [11] O. K. Andersen, Phys. Rev. B **12**, 3060 (1975); O. Gunnarsson, O. Jepsen, and O. K. Andersen, *ibid.* **27**, 7144 (1983).
 [12] F. Borgatti *et al.*, Phys. Rev. B **65**, 090406 (2002).
 [13] S. Fujii, S. Ishida, and S. Asano, J. Phys. Soc. Jpn **64**, 185 (1994).
 [14] P. Webster and M. Ramadan, JMMM **5**, 51 (1977).
 [15] P. J. Webster, J. Appl. Phys. **52**, 2040 (1981).
 [16] E. Silva, O. Jepsen, and O. Andersen, Solid State Comm. **67**, 13 (1988).
 [17] K. Buschow and P. V. Engen, JMMM **25**, 90 (1981).
 [18] R. T. D.P. Oxley and K. Williams, J. of Appl. Phys **34**, 1362 (1963).
 [19] A. S. Fujii S., Ishida S., J. Phys. Soc. Jpn. **64**, 185 (1995).

TABLE I: Structural, magnetic parameters of Heusler alloys through experimental data of [16],[17],[2],[18],[19],[4]. Calculated values of the magnetic moments are indexed with *calc.* The Fermi-level state density of Mn 3d minority-spin down states is taken from the calculated figures of the DOS respectively, eV^{-1}

alloy	struct.	a , nm	$\mu_{\text{Mn}} / \mu_{\text{Mn calc}}, \mu_B$	$\mu_X / \mu_X \text{ calc}, \mu_B$	E_f Mn 3d \downarrow , a.u.
Cu_2MnAl	$L2_1$	0.5949	3.49/3.51	0.1/-0.005	-4.6
Co_2MnAl	$B2/L2_1$	0.5756	3.01/2.847	0.50/0.684	-0.23
Co_2MnGa	$L2_1$	0.5770	3.01/2.923	0.52/0.687	-0.20
Co_2MnSn	$L2_1$	0.6000	3.58/3.420	0.75/0.864	-0.10
Co_2MnSb	$L2_1$	0.5929	3.58/3.552	0.75/0.983	0

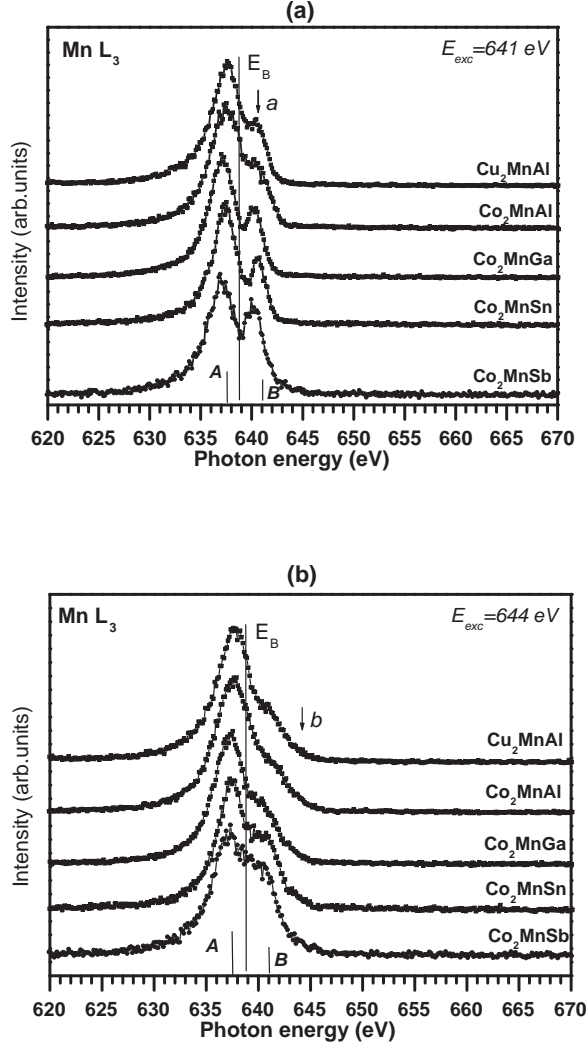


FIG. 2: Resonant x-ray emission spectra measured by excitation at the L_3 edge (a) and below the L_2 threshold. Excitation energies are indicated by the arrows and marked as a and b relative to x-ray absorption spectrum, Fig.1. The position of the Fermi level E_B is taken from the x-ray photoemission measurements of the same samples from [8], that corresponds to the Mn $2p_{3/2}$ core level binding energy. The energy position of two peaks forming the L_3 emission line are indicated as **A** and **B**

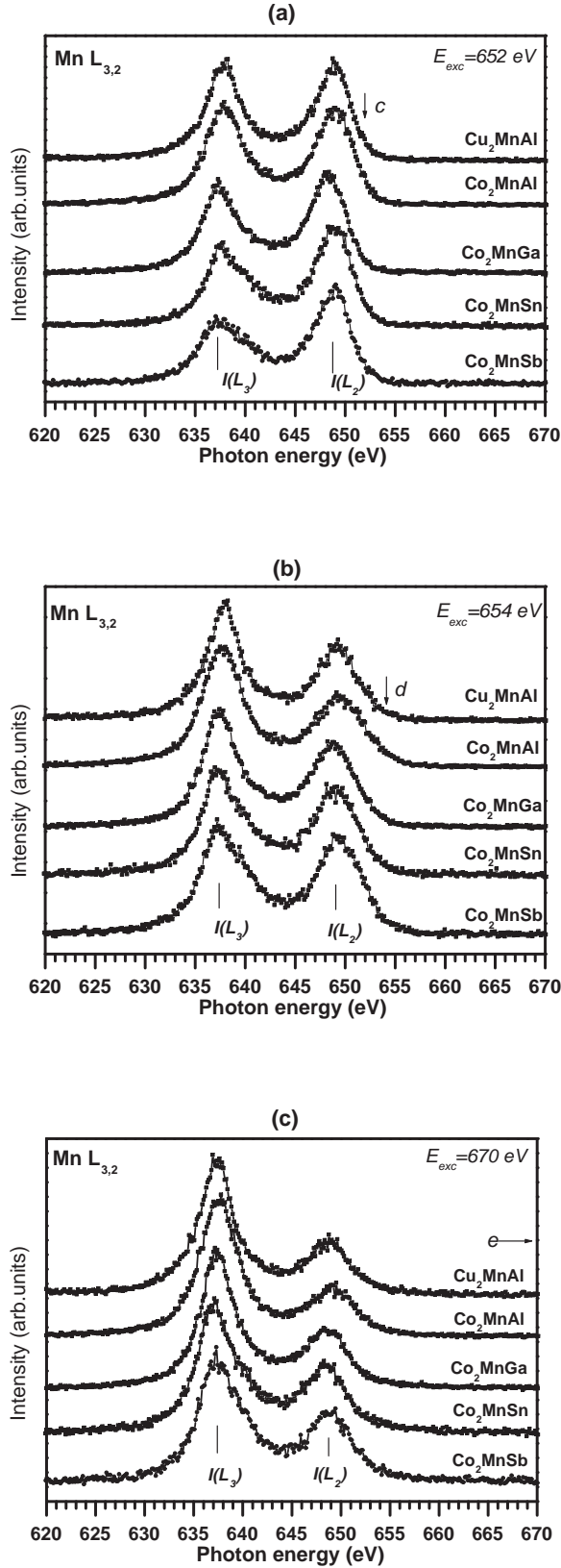


FIG. 3: Resonant x-ray emission spectra measured by excitation at the L_2 edge (a) and close to the L_2 threshold (b) toward high energy. The spectrum (c) is excited with an energy selected far from the $L_{2,3}$ absorption edges. Excitation energies are indicated by the arrows and marked as c, d and e relative to x-ray absorption spectrum, Fig.1. The energy position of the L_3 and L_2 lines are indicated as $I(L_3)$ and $I(L_2)$.

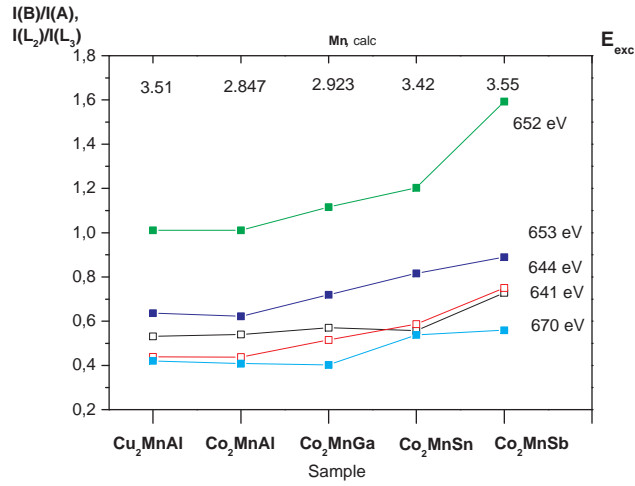


FIG. 4: Intensity ratio dependence: $I(B)/I(A)$ for 641 - 644 eV and $I(L_2)/I(L_3)$ for 652-670 eV excitation energies E_{exc} , eV. Excitation energies are at the left grid. Calculate values of μ_{Mn} are shown at the top.

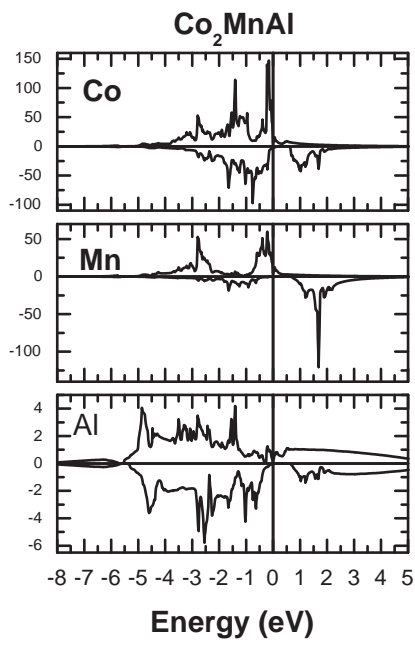
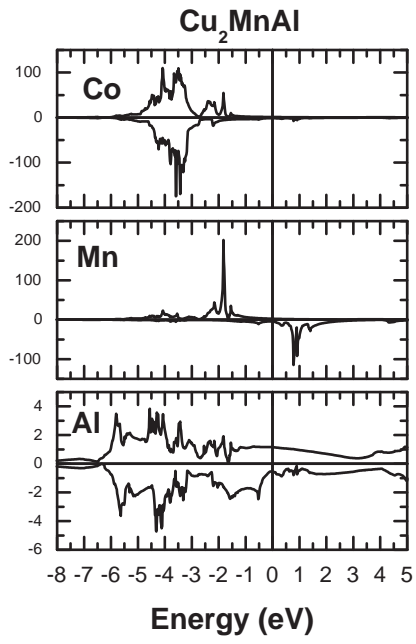


FIG. 5: Site- and spin- projected state densities of d and p electrons of the Me,Mn and Al

